CRYOGENIC TYPE-V PRESSURE VESSEL DESIGN, MANUFACTURING AND TESTING

R. Ufuk[1,2*], T. Karakaş[2], K. Bilge[3], M. Ereke[1], A. Karabeyoğlu[4]

[1] Faculty of Mechanical Eng., Istanbul Technical University, Istanbul, Turkey, ufuk@itu.edu.tr
[2] DeltaV Space Technologies Corp., Istanbul, Turkey, tkarakas@deltav.com.tr
[3] Insight Technology Development and Consultancy, Kozyatağı, Turkey, insightlabsinfo@gmail.com
[1] Faculty of Mechanical Eng., Istanbul Technical University, Istanbul, Turkey, ereke@itu.edu.tr
[4] Aerospace Engineering Dept., Koç University, Istanbul, Turkey, akarabeyoglu@ku.edu.tr

Keywords: Type-V, Cryogenic, Composite, Pressure vessel, Micromechanics

ABSTRACT

Type-V (Linerless) composite pressure vessels, which are frequently used in space applications, have an important place in launch vehicles in terms of weight. For linerless composite vessels, the composite shell should provide strength to the vessel; additionally, it should behave as a liquid and gas permeation barrier under pressure and environmental loads. One of the recent demands for pressure vessels in the space industry, is materials that are adaptable to cryogenic environment. This paper presents details of a low-cost hybrid structured linerless cryogenic composite pressure vessel development study. The study includes the fabrication methodology of the vessel, examining the concept design with hydro and cryogenic tests, and also using the multiscale finite element method. A composite case is composed of glass and carbon layers. The glass layer acts as a non-permeable barrier, and the carbon layer provides strength to the structure. The fabrication methodology for Type-V vessels is based on a liquefiable paraffin mandrel and the wet filament winding method. The paraffin-based mandrel is used with a cold-curing epoxy system, and the liquefaction process is completed in an autoclave with post-curing. The hydro leakage tests proved the structural integrity and non-permeable capability of the linerless pressure vessel for liquids; however, the tank cannot bear thermal loads under cryogenic conditions. The cryogenic thermal load damage is also observed with hydrotesting of the cryogenically tested vessel. Also, a micromechanical strategy with representative volume elements (RVE) has been utilized to understand stress distributions and damage initiation on composite structure as well as the relationship between constituent properties and large-scale (effective) properties of composite materials. All these phases are preliminary parts of the cryogenic Type-V development methodology in mechanical aspects.

1 INTRODUCTION

Type-V (linerless) cryogenic vessels have crucial importance in terms of weight aspect for space applications. Continuous developments in composite materials enable the manufacturing of these vessels with composite materials. However, cryogenic temperatures cause extreme thermomechanical effects on composite materials because of the high coefficient of thermal expansion differences between the constituents of fiber and epoxy [1–3]. Kang [4] describes vessel types according to their structure and compares them from a cost, weight, and safety perspective. Type-V tanks provide up to 60% weight savings without any reliability cost.

The objective of developing a linerless cryogenic composite tank should be examined from both a modelling, experimental, and manufacturing perspective. There are many studies in the literature that are focused specifically on manufacturing, constituent testing, or modelling. The most comprehensive work for linerless composite pressure vessels is done by Mallick et al. [5]. Their study includes material development, an analytical micromechanical approach, tank design, and finite element analysis.

The manufacturing-wise studies discuss inflatable[4], dissolvable[6], and collapsible[7] mandrel types that are applicable to Type-V tank manufacturing. The modelling wise studies focus on a multi-scaled mechanic approach where constitutive relations are of concern. The constituents as fiber, epoxy, and fiber-epoxy interactions were researched with micro- and meso-scale calculations by analytical and finite element methods [2,3,8–10].

This paper presents preliminary studies for low-cost cryogenic Type-V tank development. The study includes manufacturing method, hydro and liquid nitrogen tests for linerless tank, and micro-scale structural calculations. In the first phase, Type-V tank manufacturing was established with a liquefiable paraffin-based mandrel and wet filament winding technique. The tank has a hybrid composite structure with glass and carbon layers. The glass layers were employed to obtain a non-permeable layer. An aerospace-grade advanced epoxy system was utilized because of its cold curing capability. The manufactured tank was then hydrotested to see if there were any major leakage problems. After hydrotesting, the tank was also tested under cryogenic conditions by liquid nitrogen (LN2) filling. The LN2-tested tank is then also hydrotested again to evaluate the damage of the cryogenic temperature. The design was also evaluated with micro- and macro-level finite element analysis. By using representative volume elements, the micro and macro stress-strain levels were combined, and micro-crack initiation was investigated.

2 MATERIALS AND METHODS

2.1 Manufacturing

Standard modulus carbon fiber, E-glass fiber, and an aerospace grade cold curing epoxy system were used for manufacturing. The wet filament winding technique was used with a liquifiable mandrel, which is manufactured by casting paraffin into molds. The filament winding process was completed via a 4-axis filament winding machine. The system was cured in an autoclave at 4 bar pressure and a room temperature of 1 day, followed by an additional 4 hours at 100°C.

Paraffin was used to obtain a dissolvable mandrel for winding. A stainless steel dome with a standard 265mm inner diameter and 4mm thickness was manufactured by bending for use as a mold. The boss material is Aluminum 6061-T6. Then this paraffin based in-house manufactured mandrel was used during the wet winding process (Figure 1).

The composite layup is designed as 2 glass layers (±17.9˚, ±22.4˚), 1 carbon hoop layer (±89.8˚), and 2 helical (±11.5˚) carbon layers as a hybrid structure. These angles were chosen just to fully cover the paraffin mandrel and provide non-slippage on fibers during the winding process. Glass layers are aimed to provide a non-permeable layer.

Figure 1: Filament winding on paraffin mandrel and autoclave curing

2.2 Trans-Scale Thermomechanical Analysis Methodology

A trans-scale hierarchical analysis [2,8] is employed to understand the micromechanical stress behavior of the constituents. The microscopic stress field of a point is calculated coupled with unit stress fields based on strain response at the microscale. The same point's fiber and resin are then assessed. The following is the superposition formula[2,8]:

$$\{\sigma^u\}^e = [H]^e\{\varepsilon^M\} + \Delta T\{S\}^e \tag{1}$$

where $\{\sigma^u\}^e$ is the unit cell's microscopic stress field at particular macroscopic stresses and temperatures. $[H]^e$ is the unit microscopic stress field of a unit cell under unit strain loading produced by applying the periodic boundary conditions to a hexagonal unit cell, and $\{\varepsilon^M\}$ is macroscopic strains determined by traditional finite element analysis, which is a 6x1 column. ΔT is the change in the temperature, and $\{S\}^e$ is the stress field on the fiber-matrix scale calculated by unit thermal loading case [2,8].

The failure criteria for fiber are:

$$-X_f^C < \sigma_{f1} < X_f^T \tag{2}$$

Where X_f^C, X_f^T fibers tensile and compressive strength values, σ_{f1} is maximum axial microstress value on fiber.

The resin materials are generally isotropic, but the tensile strength T_M and compressive strength C_M can be different. According to the literature, matrix fracture is generally based on Von Mises stress σ_{vM}[2,8];

$$\sigma_{vM} \geq X_{mt} \tag{3}$$

where σ_{vM} is the equivalent Von Mises of resin, and X_{mt} is the tensile strength of resin.

2.3 Materials and Micro FE Analyses

The thermomechanical properties of the constituents have been given in Table 1 and Table 2 [2,11]. The carbon fiber is IM7, the glass fiber is E-Glass and the resin material is 977-3. These material properties have been taken from the literature and may include differences with materials that were utilized in manufacturing.

Material	E1 (GPa)	E2=E3 (GPa)	G12= G13 (GPa)	G23 (GPa)	μ23	μ12= μ13	α11 (K^{-1})	α22= α33 (K^{-1})	X_T (MPa)	X_C (MPa)
Carbon Fiber	263	19	27.6	6.9	0.35	0.2	-0.9e-6	7.2e-6	5180	3200
E-Glass Fiber	74	74	30.8	30.8	0.22	0.22	4.9-6	4.9e-6	2150	1450

Table 1: Thermo-mechanical properties of carbon fiber and E-Glass fiber

Property	@ 295K	@ 77K
E (GPa)	3.36	4.77
α (K^{-1})	56.57e-6	18.67e-6
Poisson's Ratio	0.35	0.35
Tensile Strength (MPa)	90	130

Table 2: Thermo-mechanical properties of resin

Six unit mechanical and one unit temperature loadings were performed for hexagonal a RVE with volume fraction ratio of 0.45 and micro stress distributions were obtained. These analyses have been done for glass and carbon fiber material systems with resin thermomechanical properties at 295K and 77K (Figure 2 and Figure 3). If the macro-analysis environmental load includes thermal loading, the RVE model with cryogenic material properties has been used. Otherwise, the RVE with room temperature material properties has been used. The micro-model contains 944 solid elements for the matrix region and 1136 solid elements for the fibers. Also, orthotropic material properties that were used in macro-analysis, were evaluated with these RVE elements (Table 3).

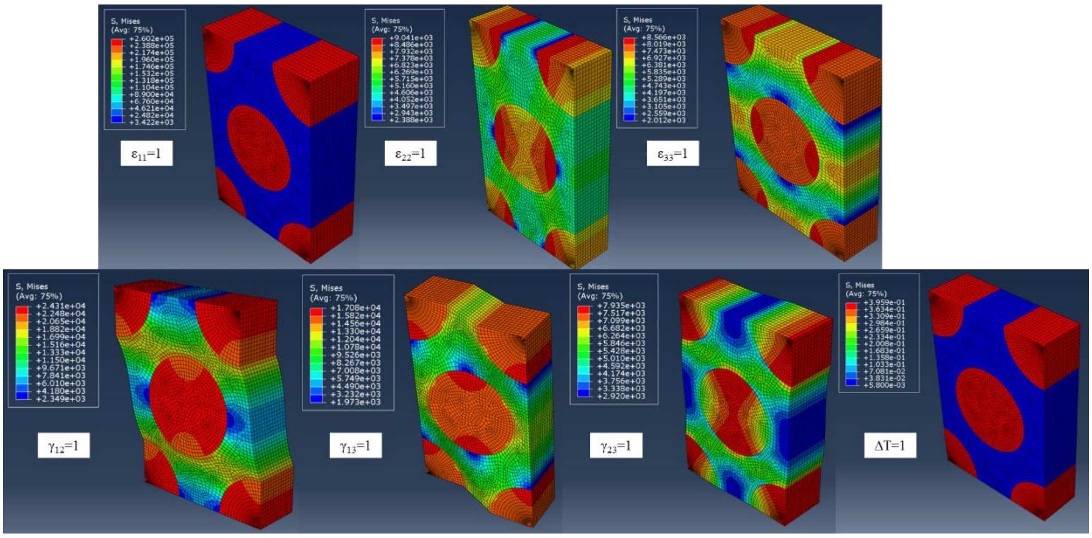

Figure 2: Von Mises stress distribution of IM7/977-3 RVE with 77K properties for unit loadings

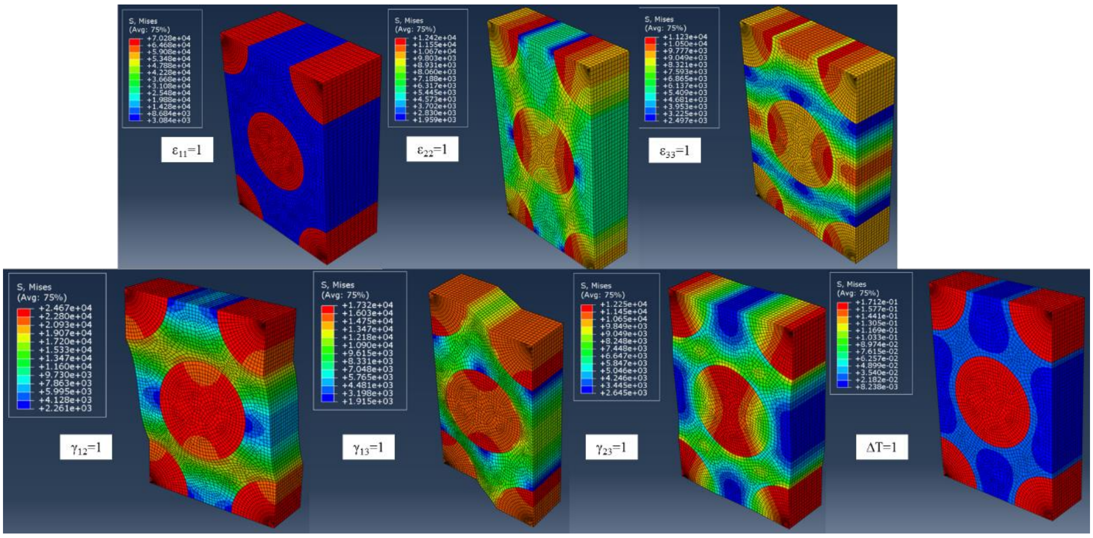

Figure 3: Von Mises stress distribution of E-Glass/977-3 RVE with 77K properties for unit loadings

2.4 Macro FE Analyses

ANSYS Workbench has been used for composite tank structural analysis. Composite layup is defined in the ACP-Pre module with filament wound layup angle and thickness data gathered via CADFIL software (Figure 4). A total of 108.734 elements as SOLID186 (Layered) for composite layers and SOLID186 for polar bosses were employed.

The cryogenic load is applied as liquid nitrogen temperature (77K) from room temperature (295K). The boundary conditions were defined as fixed support at one end and axially free at the other end. The tank has been subjected to three different loading conditions separately:

- Case 1: Hydrotest / Only +30 bar pressure
- Case 2: Cryogenic Filling/ LN2 thermal load and +5 bar pressure load
- Case 3: Only LN2 thermal load (295K to 77K)

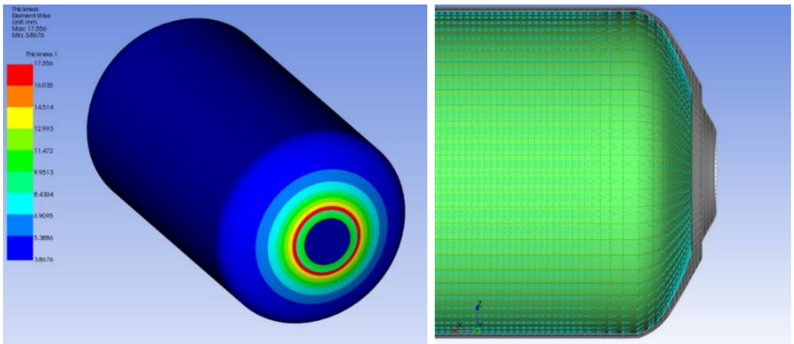

Figure 4: Composite thickness distribution and fiber angle representation

Material	IM7/ 977-3		E-Glass/ 977-3	
Property	At 295K	At 77K	At 295K	At 77K
E1 (GPa)	159.15	159.72	45.76	46.33
E2 (Gpa)	8.56	10.56	11.87	15.83
E3 (Gpa)	8.56	10.56	11.87	15.83
G12 (Gpa)	4.29	5.74	4.35	5.84
G23 (Gpa)	2.96	3.65	4.27	5.72
G31 (Gpa)	4.29	5.74	4.35	5.84
nu12	0.254	0.255	0.265	0.265
nu13	0.254	0.255	0.265	0.265
nu23	0.438	0.437	0.401	0.392
α_x (10-6/K)	-0.349	-0.642	6.622	5.544
α_y (10-6/K)	31.874	13.827	28.392	11.164
α_z (10-6/K)	31.866	13.825	28.392	11.165

Table 3: Thermo-mechanical properties of carbon and glass layers

3 RESULTS AND DISCUSSION

3.1 Case 1: Hydrotest and Micro Scale Analysis

The tank permeability was investigated via hydrotest with an in-house pressurization setup (Figure 5a). Pressurization was done by increasing the pressure level gradually, as depicted in Figure 5b, with three cycles of pressure loading and unloading. The measurements suggested that the manufactured tank can maintain the input pressure for designated hold durations without micro-cracking (Table 4). At the end of the test, the outer surface was checked by hand, and no damage or leakage was observed at the surface.

Input Pressure(bar)	Hold Duration(min)	Internal Pressure(bar)
30.2	1	27.1
29.5	1	26.2
30.3	2	25.7
30.3	4	25.7

Table 4: Hydrotest pressure values

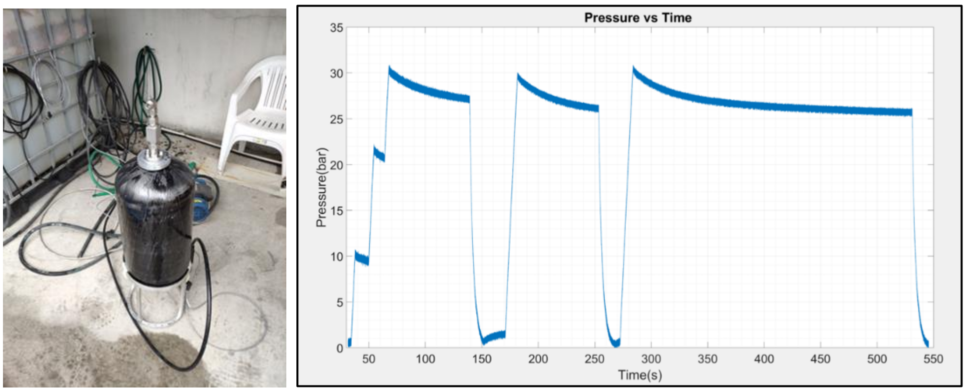

Figure 5: (a) Hydrotesting of the linerless tank, (b) Pressure-Time data during hydrotest

Also, the hydrotest case is evaluated by using trans-scale analysis on the cylindrical region (Table 5). As it can be seen from the table, none of the fiber materials exceed their tensile/compression strength values, and the Von Mises stress values of the matrix constituent are below the matrix tensile strength at room temperature (90MPa). The trans-scale analysis confirms that there is no micro-damage.

Loading Condition	Layer	Macro	Fiber - Micro		Macro	Matrix- Micro			Micro Crack
		$\sigma_{Fiber\ Direction}$ (MPa)	σ_{Max} (MPa)	σ_{Min} (MPa)	$\sigma_{Transverse\ Direction}$ (MPa)	σ_{Max} (MPa)	σ_{Min} (MPa)	σ_{Mises} (MPa)	σ_{Mises}
Only +30 bar pressure	Glass (±17.9˚)	45.3	173.8	-5.8	35.5	132.1	-15.1	33.3	No
	Glass (±22.4˚)	50.6	178.6	-5.4	34.5	79.4	-15.4	33.4	No
	Carbon (±89˚)	491.3	803.2	-0.6	10.5	119.5	-6.5	26.6	No
	Carbon (±11.5˚)	117.1	177.1	-2.4	26.3	66.5	-8.9	23.8	No
	Carbon (±11.5˚)	119.4	183.1	-2.6	26.1	112.6	-8.9	26.1	No

Table 5: Trans-Scale results of Case 1: Hydrotest

3.2 Case 2: Cryogenic Filling and Micro Scale Analysis

The cryogenic test of the Type-V pressure vessel was conducted via LN2 filling (Figure 6a, 6b). During the filling process, a debonding event was captured in the metal/composite interface on the polar boss region. This type of failure was expected due to the high CTE difference between the aluminum polar boss and composite shell. As can be seen from Figure 7, the pressure value increased to 10 bar while the filling process started, then ventilation was opened, and the pressure value started to decrease (average 5 bar during the test). After LN2 leakage was noticed, the filling process stopped, ventilation was fully opened, and test was stopped.

The trans-scale analysis details of the cryogenic filling case on the cylindrical region have been given in Table 6. The fiber stress values and matrix Von Mises stress values are below strength limits, and damage is not expected according to Von Mises criteria. However, the resin material loses its ductility under cryogenic conditions and becomes brittle, and this situation requires changing the failure criteria to maximum stress criteria for matrix, which will give much more correct results. The matrix maximum stress values are higher than the tensile strength of the resin material on the glass layers and close to the tensile strength of the resin material on the carbon layers, which indicates micro failure on the matrix.

Figure 6: (a) Cryogenic testing setup, (b) Cryogenic Filling

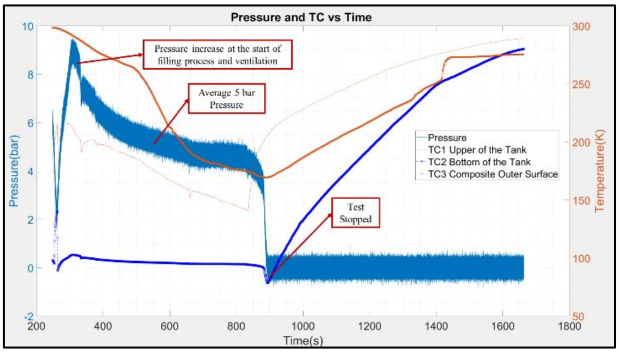

Figure 7: Pressure and temperature values versus time

Loading Condition	Layer	Macro σ_{Fiber} Direction (MPa)	Fiber - Micro σ_{Max} (MPa)	Fiber - Micro σ_{Min} (MPa)	Macro $\sigma_{Transverse}$ Direction (MPa)	Matrix- Micro σ_{Max} (MPa)	Matrix- Micro σ_{Min} (MPa)	Matrix- Micro σ_{Mises} (MPa)	Micro Crack $\boldsymbol{\sigma_{Max}}$
LN2 Thermal load and +5bar pressure load	Glass (±17.9˚)	58.1	280.5	-6.5	37.2	156.8	-11.1	35.1	Yes
	Glass (±22.4˚)	57.2	277.7	-6.4	37.1	156.6	-10.9	35	Yes
	Carbon (±89˚)	-92.9	130.2	-206.5	28.8	128.2	-6.8	25.7	On Limit
	Carbon (±11.5˚)	-41.5	127	-121.8	26	126.2	-5.8	22.7	On Limit
	Carbon (±11.5˚)	-42.5	126.8	-121.4	25.7	126.1	-5.8	22.6	On Limit

Table 6: Trans-Scale results of Case 2 Cryogenic Filling

3.3 Case 3: Only LN2 thermal load (295K to 77K) and Micro Scale Analysis

The trans-scale analysis is also conducted for the case of only LN2 thermal load on the cylindrical region to understand the thermal load effect clearly (Table 7). The above mentioned ductile-brittle transition is again valid for this case, which indicates failure on glass and carbon hoop layers with only LN2 thermal load (Table 7). Also, the comparison of the values between Table 5 and Table 7 depicts that the LN2 thermal load-caused stress values are close to the 30 bar pressure load ones on the glass and carbon hoop layers; however, they are higher by around 50 percent on the helical carbon layer.

Loading Condition	Layer	Macro $\sigma_{Fiber\ Direction}$ (MPa)	Fiber - Micro σ_{Max} (MPa)	Fiber - Micro σ_{Min} (MPa)	Macro $\sigma_{Transverse\ Direction}$ (MPa)	Matrix- Micro σ_{Max} (MPa)	Matrix- Micro σ_{Min} (MPa)	Matrix- Micro σ_{Mises} (MPa)	Micro Crack $\boldsymbol{\sigma_{Max}}$
Only LN2 thermal load (295K to 77K)	Glass (±17.9˚)	50.1	268.7	-8.7	29.9	151.6	-8.1	31.1	Yes
	Glass (±22.4˚)	48.6	265.6	-9.4	30.1	151.7	-8.1	31.2	Yes
	Carbon (±89˚)	-166.9	128.6	-327.5	26.6	126.3	-6.2	25.6	On Limit
	Carbon (±11.5˚)	-60.8	86.1	-185.8	21.2	90.3	-9.5	38.6	No
	Carbon (±11.5˚)	-62.3	86.5	-187.2	20.9	90.7	-9.3	38.1	No

Table 7: Trans-Scale results of Only LN2 thermal load (295K to 77K)

3.4 Hydrotest after Liquid Nitrogen (LN2) Test

The LN2-tested tank was hydrotested to see the effect of cryogenic thermal load on composite damage and permeability. During the hydrotests, the composite layup sweats the water with a 4-5 bar pressure load (Figure 8). The thermal load with LN2 caused thickness through microcrack accumulation, and the composite layup lost its non-permeability.

The trans-scale analysis with maximum stress criterion on matrix accurately foreseen this damage on the composite shell under LN2 thermal load. However, the Von Mises criterion has false premises for thermal load cases in terms of matrix crack initiation.

Figure 8: Leakage of composite after LN2 test.

4 CONCLUSIONS

In conclusion, this study on the development of a low-cost cryogenic Type-V tank has significant practical implications for the space industry that require efficient and affordable cryogenic storage solutions. The utilization of a liquefiable paraffin mandrel and wet filament winding technique demonstrated promising results in the manufacturing process, paving the way for cost-effective tank production.

The hydrotest conducted in the initial phase confirmed the integrity of the tank design, as no major leakage was observed. Complementing this, trans-scale finite element analysis provided further validation. However, during the cryogenic LN2 filling, the presence of a high thermal expansion difference between the composite case and the aluminum polar boss led to interface debonding at the halfway point. The LN2-tested tank was hydrotested again to see if there was damage to the permeability of the composite case. The composite case was sweated at 4-6 bar pressure values from all surfaces. The high temperature difference caused major damage to the composite case, and the microcracks formed and accumulated through thickness. The trans-scale analysis cannot capture this failure according to Von Mises stress criteria. As a result, it is required to use maximum stress criterion under cryogenic conditions because of the ductile brittle transition of the resin material under cryogenic conditions. The maximum stress criterion gives correct results and correctly points failure on glass layers and also points that the carbon layers were reached their limit. Also, it should be pointed that the manufacturing-related uncertainties can significantly affect in-situ strength levels of the matrix on a micro-scale.

Speaking about limitations of this study, one of them is that the calculation method determines only the first crack failure; the calculation method should be improved with progressive damage analysis on a micro-scale level. The stress-based damage method could be improved to include energy-based damage criteria, and interface strength should also be evaluated.

Another problem that should be investigated is the thermal gradient through thickness during cryogenic liquid filling. The inner side faces LN2 while the outer surface interacts with air, which causes a thermal gradient through thickness, which shows the requirement of determining crack evolution through thickness.

At the end, this study provided informative details about manufacturing, testing, and analyzing methods for developing a low-cost cryogenic Type-V tank.

ACKNOWLEDGEMENTS

The authors greatly acknowledge DeltaV Space Technologies Inc. for financial support and providing research facilities for the realization of this study.

REFERENCES

[1] Mallick, K., Tupper, M. L., Arritt, B. J., and Paul, C. Thermo-Micromechanics of Microcracking in a Cryogenic Pressure Vessel. No. 5, pp. 3320–3329.

[2] Huang, C., Ren, M. F., Li, T., Chang, X., Cong, J., and Lei, Y. J. "Trans-Scale Modeling Framework for Failure Analysis of Cryogenic Composite Tanks." *Composites Part B: Engineering*, Vol. 85, 2016, pp. 41–49. https://doi.org/10.1016/j.compositesb.2015.09.023.

[3] Peddiraju, P., Lagoudas, D., Noh, J., and Whitcomb, J. Numerical Modeling of Cryogen Leakage through Composite Laminates. No. 5, pp. 3761–3771.

[4] Kang, H. min, and Lee, J. K. Linerless Pressure Vessel by Centrifugal Forced Weaving and Method for Manufacturing Thereof, US 2015/025874.0 A1, 2014.

[5] Mallick, K., Cronin, J., Ryan, K., Arzberger, S., Munshi, N., Paul, C., and Welsh, J. S. "An Integrated Systematic Approach to Linerless Composite Tank Development." *Collection of Technical Papers - AIAA/ASME/ASCE/AHS/ASC Structures, Structural Dynamics and Materials Conference*, Vol. 5, 2005, pp. 3553–3569. https://doi.org/10.2514/6.2005-2089.

[6] Kaerger, J., and Atz, L. Water Soluble Mandrels for Lost Core Applications in Manufacturing of Hollow Composite Structures. 2019.

[7] Brooks, J. C. Method Fabricating a Collapsible Mandrel Structure to Be Used in Manufacturing Reinforced Hollow Tanks, 4,684,423, 1987.

[8] Ren, M. fa, Zhang, X. wen, Huang, C., Wang, B., and Li, T. "An Integrated Macro/Micro-Scale Approach for in Situ Evaluation of Matrix Cracking in the Polymer Matrix of Cryogenic Composite Tanks." *Composite Structures*, Vol. 216, 2019, pp. 201–212. https://doi.org/10.1016/j.compstruct.2019.02.079.

[9] Jin, K. K., Huang, Y., Lee, Y. H., and Ha, S. K. "Distribution of Micro Stresses and Interfacial Tractions in Unidirectional Composites." *Journal of Composite Materials*, Vol. 42, No. 18, 2008, pp. 1825–1849. https://doi.org/10.1177/0021998308093909.

[10] Choi, S., and Sankar, B. V. "Micromechanical Analysis of Composite Laminates at Cryogenic Temperatures." *Journal of Composite Materials*, Vol. 40, No. 12, 2006, pp. 1077–1091. https://doi.org/10.1177/0021998305057365.

[11] Kaddour, A. S., and Hinton, M. J. "Input Data for Test Cases Used in Benchmarking Triaxial Failure Theories of Composites." *Journal of Composite Materials*, Vol. 46, Nos. 19–20, 2012. https://doi.org/10.1177/0021998312449886.